Polymer Journal (2010) 42, 555–561

www.nature.com/pj

ORIGINAL ARTICLE

SBR/silica composites modified by a polymerizable protic ionic liquid

Yanda Lei, Zhenghai Tang, Baochun Guo and Demin Jia

A novel functionalized ionic liquid, 1-methylimidazolium sorbate (MimS), was synthesized and characterized. MimS was used to improve the performance of rubber/silica composites. Substantiated hydrogen bonding between MimS and silica was responsible for effectively restraining the Payne effect and decreasing the Mooney viscosity of the uncured rubber compounds. The reactivity of MimS toward rubber and its ability to hydrogen bond with polymerized MimS and silica were characterized. Filler networking, curing behavior, silica dispersion and mechanical performance of the vulcanizates were fully studied. Remarkable improvements in mechanical properties were achieved with only a small addition of MimS. Variations in rubber performance were attributed to the significantly improved silica dispersion and novel interfacial interactions induced by MimS.
Polymer Journal (2010) **42,** 555–561; doi:10.1038/pj.2010.43; published online 26 May 2010

Keywords: interface; ionic liquid; rubber; silica

INTRODUCTION

Silica has been extensively studied for its effective reinforcing ability in rubbers. Its high polar surface (up to 8 silanol groups per nm^{2} [1]) is an important factor in determining its reinforceability.[2–4] However, its intrinsic high polar surface also leads to serious aggregation. To obtain better mechanical performance, fine dispersion of silica is generally necessary. Various methods of modifying the silica surface, therefore, are always of great importance in tailoring filler dispersion and interfacial interactions for rubber/filler composites.[5–8]

Ionic liquid (IL), a novel emerging medium, is getting worldwide attention for its fascinating properties, such as near-zero vapor pressure, high thermal stability, high conductivity and wide potential window.[9,10] Traditionally, ILs with various inorganic anions have been extensively used as green solvents (electrolyte and dispersing agents) owing to their high thermal stability, non-flammability and non-volatility. For example, 1-butyl-3-methylimidazole hexafluorophosphate has been widely used as an electrolyte in electrochemistry,[11] as a novel dispersant for carbon nanotubes[12,13] and as a medium for synthesizing nanoparticles.[14–16] When ILs are used to synthesize nanoparticles, besides as the reaction medium, they also have an important role in directing the structure of the particles.[17–20]

Previously, we verified 1-butyl-3-methylimidazole hexafluorophosphate as an effective modifier for improving the performance of rubber/halloysite nanotube composites.[21] This phenomenon is due to the hydrogen bonding between 1-butyl-3-methylimidazole hexafluorophosphate and the halloysite nanotube. However, most of the commercial ILs, such as 1-butyl-3-methylimidazole hexafluorophosphate, could not be directly used as the modifier for polymer composites because of their high polarity and limited compatibility.[22–24] Functional and compatible ILs should be specifically designed for rubber compounds. In the present work, based on the reactivities of sorbic acid and its salt towards diene rubber,[25–27] a functional IL, MimS, was synthesized and verified by ^{1}H nuclear magnetic resonance and Fourier transform infrared (FTIR) spectroscopy. MimS was investigated as a modifier for improving the performance of silica-filled styrene butadiene rubber (SBR) composites. The effects of MimS on filler networking, vulcanization behavior, mechanical performance and morphology were fully studied. The interfacial interactions induced by MimS were revealed and found to be correlated with the changes in rubber performance.

EXPERIMENTAL PROCEDURE

Materials

N-methylimidazole and sorbic acid, with 99% purity, were purchased from Alfa Aesar, Tianjin, China. SBR, with the trade name SBR1502 (styrene content 23.5 wt.%), was manufactured by Jilin Chemical Industry Company, Jilin, China. Precipitated silica, with the trade name WL180, was manufactured by NanPing Jialian Chem. Ltd., Nanping, China. By using Micromeretics ASAP 2020, the Brunauer–Emmett–Teller (BET) value of silica was re-determined to be 200 $m^{2}\,g^{-1}$. Other rubber additives were industrial grade and were used as received.

Synthesis of MimS and the preparation of model compounds with MimS

Synthesis of MimS and its polymerization. The synthesis of MimS, which is similar to the synthesis of other protic ionic liquids,[28–31] and its polymerization are shown in Scheme 1.

Department of Polymer Materials and Engineering, South China University of Technology, Guangzhou, PR China
Correspondence: Dr B Guo, Department of Polymer Materials and Engineering, South China University of Technology, Guangzhou 510640, PR China.
E-mail: psbcguo@scut.edu.cn
Received 1 March 2010; revised 30 March 2010; accepted 12 April 2010; published online 26 May 2010

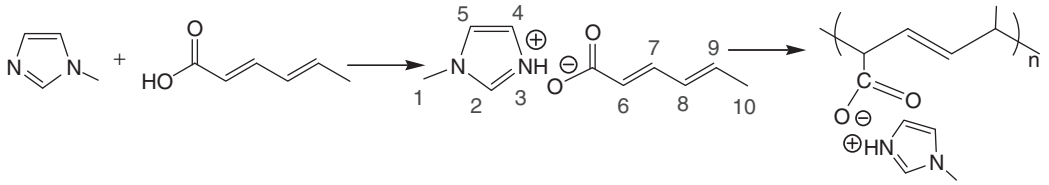

Scheme 1 Synthesis of MimS and its polymerization.

N-methylimidazole and sorbic acid were stoichiometrically reacted at 35 °C, with stirring, for 1 h, which yielded a light yellow transparent product. This product was characterized by FTIR spectroscopy (Bruker Vertex 70 FTIR spectrometer; Bruker, Buchen, Germany) and ^{1}H nuclear magnetic resonance (Bruker AVANCE Digital nuclear magnetic resonance spectrometer; Bruker, 300 MHz). ^{1}H nuclear magnetic resonance ($CDCl_3$, 300 MHz):[32–35] 12.34(s, 1H, H(3)); 7.65(s, 1H, H(2)); 7.23–7.32(m, 1H, H(7)); 7.09–7.10(t, J_1=1.11 Hz, J_2=1.35 Hz, H(4)); 6.880–6.884(d, J=1.23, 1H, H(5)); 6.17–6.21(m, J=10.59 Hz, 1H, H(8)); 6.12–6.14(m, H(9)); 5.79–5.84(d, J=3.70 Hz, 1H, H(6)); 3.07(s, 3H, H(1)); 1.83–1.86 (d, J=6.45 Hz, 3H, H(10)). FTIR (KBr):[36–40] 3414(N–H), 3125(imidazole–H), 3024 and 1000 (C=C–C=C–H), 1690 (C=O), 1420 (C–O), 1650 (C=C in imidazolium cation). Anal. calculated for MimS ($C_9H_{14}O_2N_2$): C 61.79, N 14.42, H 7.21. Found: C 60.59, N 14.43, H 8.18. The melting point and the melting heat were 16.5 °C and 15.2 kJ mol^{-1}, respectively. The viscosity was 105 mPa s (25 °C). Bulk polymerization of MimS was conducted with 2,2′-azobisisobutyronitrile (1 wt.%) as the initiator under a nitrogen atmosphere. Polymerized MimS (poly(MimS)) was characterized by FTIR spectroscopy.

MimS/silica interaction. The silica was dispersed in MimS under sonication, and the resultant suspensions were subjected to centrifugation to test the formation of the MimS/silica gel. X-ray photon spectroscopy (Kratos Axis Ultra DLD; Kratos Analytical, Eppstein, Germany) was performed on the silica and the MimS-coated silica to reveal the interaction between them. The binding energy for each spectrum was calibrated to its C1s reference at 285.0 eV. A Gaussian function was used in the fitting program.[41]

Polymerized MimS in the presence of silica and grafting of MimS onto SBR. To verify the affinity of MimS towards silica and its reactivity towards SBR chains, polymerization assays were conducted. Polymerization of MimS in the presence of silica was conducted following the procedure described above. Grafting copolymerization of MimS onto SBR was performed in a toluene solution of SBR with 2,2′-azobisisobutyronitrile as the initiator. The weight ratio of SBR/MimS/2,2′-azobisisobutyronitrile was 10/5/0.15. All polymerizations were conducted at 70 °C for 12 h. The MimS grafted SBR (poly(SBR-g-MimS)) was extracted with plenty of deionized water to remove poly(MimS). Poly(MimS)/silica and poly(SBR-g-MimS) were verified by FTIR spectroscopy. Differential scanning calorimetry experiments were performed on poly(MimS) and poly(MimS)/silica to explore the possible interactions between poly(MimS) and silica. The samples were heated from −85 to 20 °C at 10 °C min^{-1} with nitrogen as the purging gas.

Preparation of SBR/silica compounds

SBR and other additives were mixed on an open two-mill moll. The composition (in per hundred parts of rubber, p.h.r.) was as follows: SBR 100, silica 40, zinc oxide 5, stearic acid 1, dicumyl peroxide 1, *N*-isopropyl-*N*′-phenyl-p-phenylenediamine 1.5 and MimS variable. The dependence of shear modulus (G') on the strain of uncured rubber compounds was measured using visco-elastography rubber processing analyzer (Göttfert-Werkstoff-Prüfmaschinen GmbH, Ahlden, Germany). The temperature and frequency were set to 70 °C and 1 Hz, respectively. The Mooney viscosity was determined following ISO standard 289-2005 at 100 °C. In the below text, R**x**MimS means the rubber sample with **x** p.h.r. MimS.

The curing characteristics of the rubber compounds were determined using a UR-2030 vulcameter (U-CAN, Nantou, Taiwan) at 170 °C. Then, the rubber compounds were vulcanized at 170 °C×Tc90. Tensile, tear and hardness tests of the vulcanizates were performed following ISO 37-2005, ISO 34-2004 and ISO 7619-2004, respectively. Dynamic mechanical analysis of the vulcanizates was performed on an EPLEXOR dynamic mechanical analyzer (Gabo Qualimeter Testanlagen GmbH, Ahlden, Germany). The samples were scanned from −100 to 100 °C at 3 °C min^{-1}. The tensile mode was adopted. Cross-link densities of the vulcanizates were determined using the equilibrium swelling method.[42]

Scanning electron microscopy was performed for cryogenically fractured vulcanizates with a LEO 1530 VP scanning electron microscope (LEO Elektronenmikroskopie GmbH, Oberkochen, Germany). Before the observations, a thin layer of gold was sprayed on the fractured surface. Transition electron microscopy observations were performed on slices generated with an ultra microtome (~200 nm) using a Philips Tecnai 12 transmission electron microscope (Philips, Eindhoven, Netherlands) with an accelerating voltage of 30 kV.

RESULTS AND DISCUSSION

Interaction between MimS and silica

To verify the interaction between MimS and silica, the silica/MimS mixture was subjected to sonication and centrifugation. As revealed in Figure 1, the silica/MimS gel was generated, indicating a strong interaction between MimS and silica. Having been washed by acetone and centrifuged, the vacuum-dried samples were characterized by X-ray photon spectroscopy, as shown in Figure 2. The Si atoms were present in two chemical environments: SiOH (105.0 eV) and SiOSi (103.7 eV).[43] However, after being centrifuged and vacuum dried, no silanol group was found according to the fitting program. We propose that SiOH, after interacting with the anion, decreased the binding energy value of the related Si atom. The binding energy value of the Si atom in SiOSi increased for the hydrogen bonding between SiO and the cation in MimS. As a result, the binding energy value for Si atoms in the two environments overlapped and could not be easily distinguished by the fitting program.

Effect of MimS on filler networking in uncured rubber compounds

Silica networks in MimS containing rubber compounds were studied by the dependence of the shear modulus (G') on strain (Figure 3). Conventionally, there is a high modulus at small strain (<1%), which mainly contributes to the production of the filler network. For increasing strain, G' does not show a linear decrease and drops to a low value. This phenomenon is related to the filler network in the rubber matrix and is termed the Payne effect.[4,6,44] The shear modulus

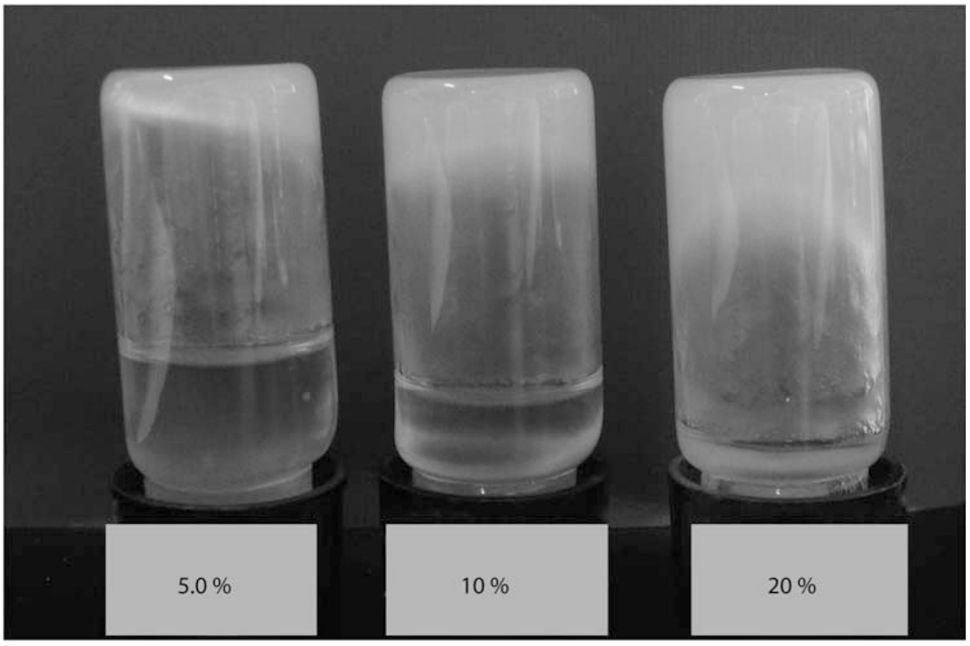

Figure 1 Silica/MimS gel with different weight ratios. A full color version of this figure is available at *Polymer Journal* online.

discrepancy ($\Delta G'$) between G' at small strain ($\sim$0.5%) and G' at large strain ($\sim$100%) is always used to estimate the filler network in filled rubber compounds. As shown in Figure 3, with increasing MimS, $\Delta G'$ consistently decreased, implying that the silica network was effectively restrained and that filler dispersion improved. The restrained silica network was ascribed to a strong interaction between MimS and silica, which was substantiated above.

Keeping in mind that the filler network was restrained, the processability of the rubber compounds, which is essential for rubber compounding, was also estimated by the Mooney viscosity, which was firstly decreased from 104 (R0MimS) to 74 (R1MimS) and further decreased to 63 (R4MimS). It can be seen that with increasing MimS loading, the Mooney viscosity dramatically decreased. The Mooney viscosities of R3MimS and R4MimS decreased substantially by about 40% as compared with R0MimS. This could be related to the decreased effective filler volume originating from the restrained filler network.[6] Our report on the greatly improved processability of rubber compounds by functional IL suggests that functional ILs could potentially be applied as safe, green process ingredients to substitute for cancerigenic, polycyclic, aromatic hydrocarbons and their derivatives.[45–47]

Reactivity of MimS on SBR and the interaction between poly(MimS) and silica

Many researchers, including us, have confirmed the polymerizability of sorbyl substances such as sorbic acid and sorbates.[25–27,48–50] Although the reactivity of sorbyl in MimS should be different from sorbic acid, it is believed that it can undergo polymerization via the free radical mechanism. The polymerization of MimS was characterized by FTIR spectroscopy (Figure 4). The stretching mode of C=O around 1690 cm^{-1} could be related to the anion of MimS, which is supposed to be unconsumed during polymerization.[38] The relatively reduced absorption of the diene group around 1650 cm^{-1} indicated the polymerization of the diene group in the anion.

The reactivity of MimS on SBR chains was also revealed. The FTIR spectrum of poly(SBR-g-MimS) is shown in Figure 5. The presence of aromatic hydrogen ($\sim$3060 and $\sim$3020 cm^{-1}), CH_2 (2912 and

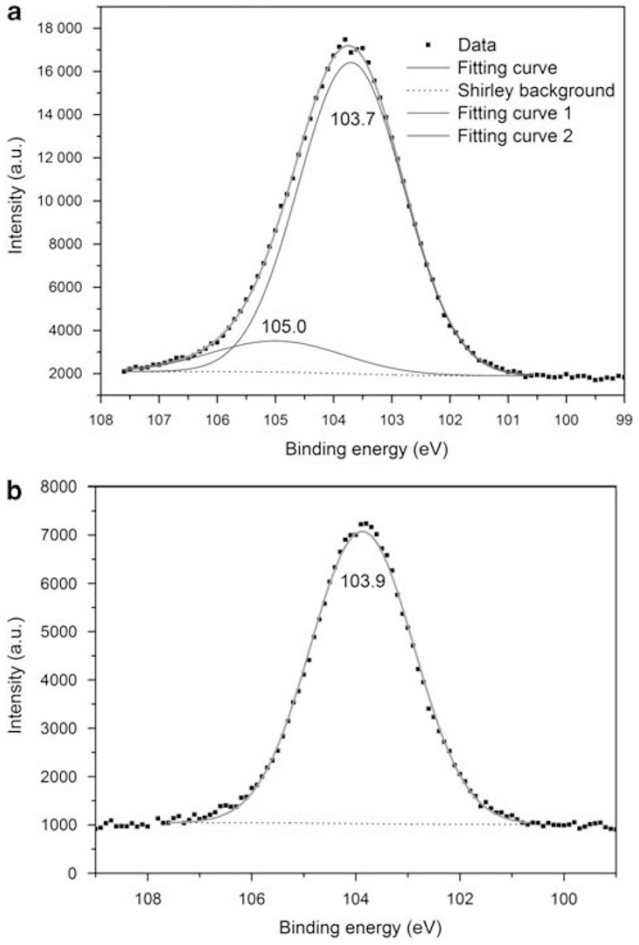

Figure 2 XPS spectra of silica (**a**) and centrifuged silica (**b**). A full color version of this figure is available at *Polymer Journal* online.

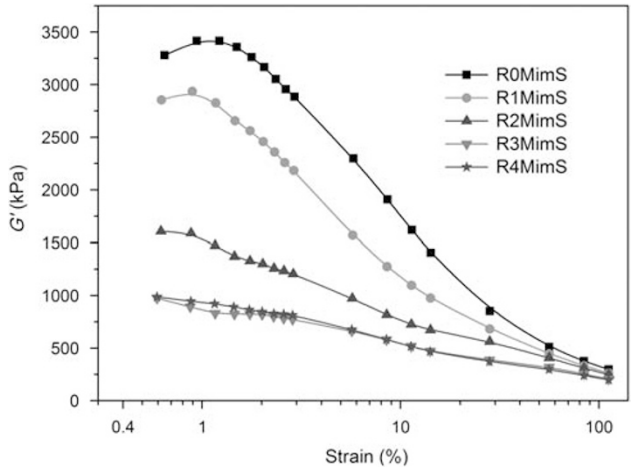

Figure 3 Strain dependence of G' of the SBR/silica compounds. A full color version of this figure is available at *Polymer Journal* online.

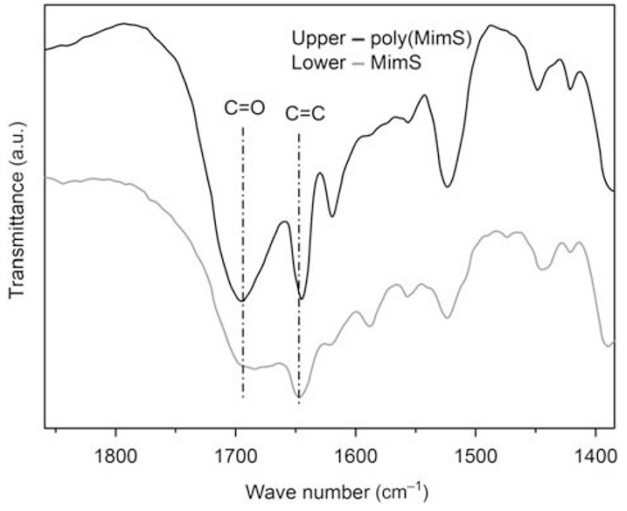

Figure 4 FTIR spectra of MimS and its polymerization product. A full color version of this figure is available at *Polymer Journal* online.

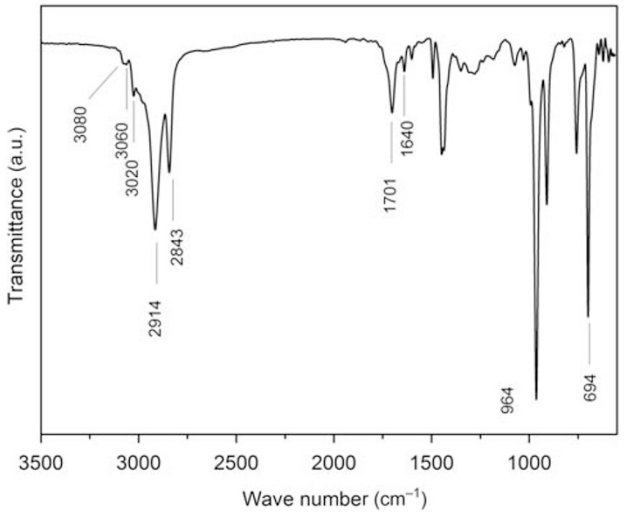

Figure 5 FTIR spectrum of poly(SBR-g-MimS).

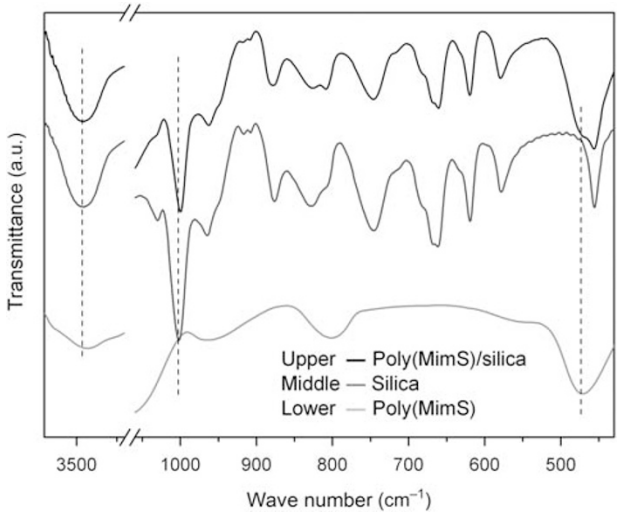

Figure 6 FTIR spectra of silica, poly(MimS) and poly(MimS)/silica. A full color version of this figure is available at *Polymer Journal* online.

2843 cm^{-1}), *trans* C=C**H** (964 cm^{-1}) and phenyl (694 cm^{-1}) indicate the backbone of SBR.[51,52] The stretching mode of aromatic C=C**H** at 3080 cm^{-1} and the stretching mode of C=C in imidazole at 1640 cm^{-1} indicate the presence of the imidazole cation on the graft product poly(SBR-g-MimS). The stretching mode of C=O at 1701 cm^{-1} [38,40] could be ascribed to the carboxyl anion. Consequently, it was verified that during vulcanization, MimS was grafted onto SBR chains.

Possible interactions between poly(MimS) and silica were verified via the model compound (poly(MimS)/silica), which was prepared by polymerization of MimS in the presence of silica (10 wt% relative to MimS). The FTIR spectra of poly(MimS)/silica and silica are presented in Figure 6. It can be seen that the peaks around 3425, 1100 and 470 cm^{-1} should be related to the silanol groups and Si–O bonds.[53] Although the adsorption of Si–O bonds on poly(MimS)/silica overlapped with the bands for poly(MimS), the shift of C–N in the imidazole ring ($\sim$1000 cm^{-1}) could be used to examine the interactions related to the imidazolium cation.[20] It is observed that the C–N stretching is blue shifted from 1002 to 999 cm^{-1}, indicating hydrogen bonding between the cation of poly(MimS) and the Si–O bond of silica. Simultaneously, the stretching mode of the silanol group above 3000 cm^{-1}, which overlaps with that of the N–H bonds in MimS, shows a relatively weak absorption and is shifted from 3414 to 3460 cm^{-1}, indicating that hydrogen bonding occurs between the silanol group (SiOH) and the carboxylic anion (COO^-) in poly (MimS), which is in agreement with another report.[20] The absorption strength of the silanol groups above 3000 cm^{-1} was reduced due to surface anchoring of poly(MimS) molecules by silica.

As the disclosed interaction between poly(MimS) and silica may affect the mobility of polymer chains, the glass transition of poly (MimS) and poly(MimS)/silica was measured by differential scanning calorimetry. According to the differential scanning calorimetry curves (not shown), the glass transition temperature (Tg) shifted from −68 °C for poly(MimS) to −64 °C for poly(MimS)/silica. The higher Tg implies that the presence of silica could effectively restrain the mobility of the polymer chains. This phenomenon may be due to hydrogen bonding between silica and poly(MimS).

Vulcanization behavior of SBR/silica compounds

Curing curves of the rubber/silica compounds are shown in Figure 7. It can be seen that with increasing MimS incorporation, the minimum

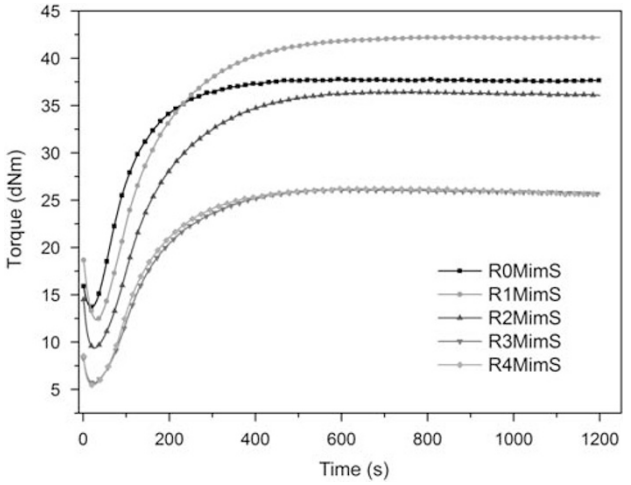

Figure 7 Vulcanization curves of the SBR/silica rubber compounds. A full color version of this figure is available at *Polymer Journal* online.

torque (T_{min}) is greatly reduced. We suggested that the restrained silica network could decrease the effective filler volume and may be responsible for the phenomenon. The maximum torque (T_{max}) during vulcanization, however, took a maximum value for R1MimS and then obviously decreased. To explain this interesting phenomenon, several factors should be considered. First, incorporation of MimS may suppress adsorption of dicumyl peroxide on the silica surface. Second, the polymerization of MimS may consume part of dicumyl peroxide. Last but not least, the altered filler network mentioned above may exert a significant influence on T_{max}. The cross-link density (Ve) for R0MimS–R4MimS is 3.32, 3.40, 3.13, 2.96 and 2.61×10^{-4} mol cm^{-3}, respectively. This may have resulted from the altered initiating efficiency of dicumyl peroxide due to the first two factors. The gradually restrained Payne effect may lower T_{max}.

Morphology observations of SBR/silica vulcanizates

The morphology of SBR/silica composites was studied by scanning electron microscopy and transition electron microscopy. As shown in Figure 8, silica is uniformly dispersed in the rubber matrix. The average size of the aggregates is much smaller than the sizes of those in the R0MimS sample. Both scanning electron microscopy and transition electron microscopy indicated that the dispersion of silica in the rubber matrix obviously improved. Two factors may be responsible for these changes in morphology. First, the polarity of the silica particles decreased due to hydrogen bonding with MimS. Second, the double bond in MimS reactive toward rubber chains might enhance interfacial bonding by the chemical bond via the radical mechanism, as substantiated above.

Mechanical performance of the SBR/silica vulcanizates

The mechanical properties of the modified SBR/silica vulcanizates are shown in Figure 9. It can be seen that the mechanical performance was substantially changed. When 4 p.h.r. of MimS was used, the tensile strength and tear strength increased by 43 and 47%, respectively. This improved mechanical strength may be due to a combination of effects, such as the improved dispersion of silica and the improved interactions between silica and the ionic unit via hydrogen bonding. As shown in Figure 9, hardness decreased slightly with an increasing load of MimS. The reduction of hardness may be related to reduced cross-linking density and the restrained filler network when sufficient MimS was used.

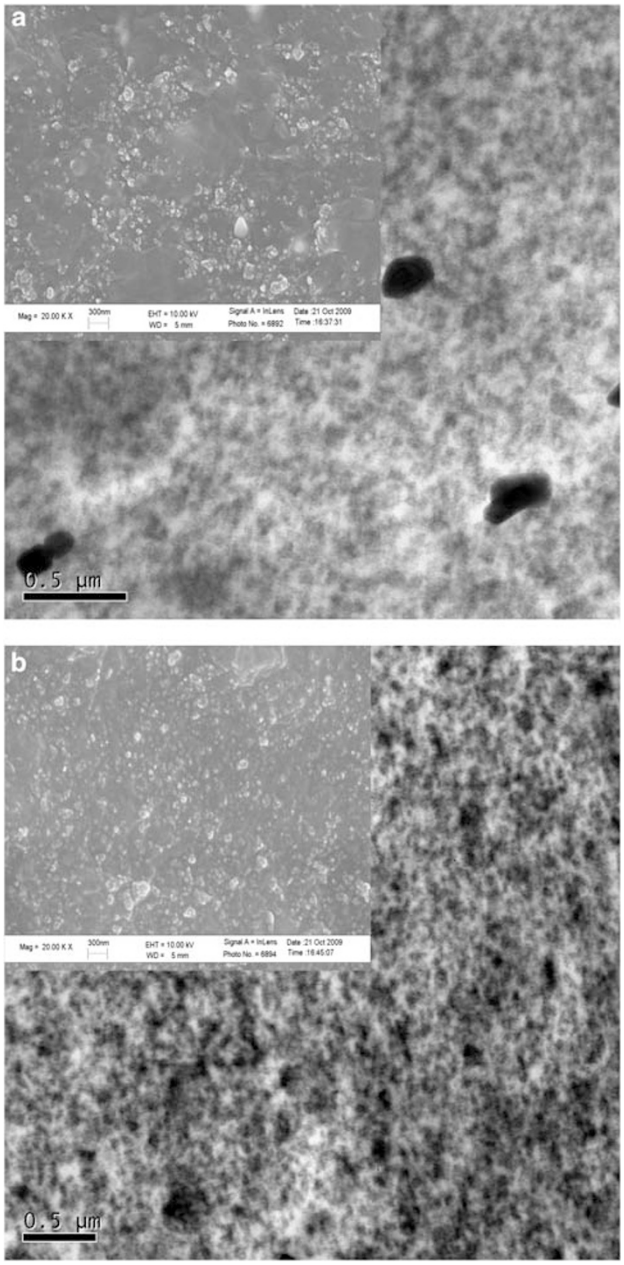

Figure 8 Morphology of R0MimS and R4MimS vulcanizates (the insets are SEM photographs).

The modulus (studied by the stress at 300%) for the samples first decreased from 7.39 MPa (R0MimS) to 6.21 MPa (R1MimS) and further decreased to 5.35 MPa (R4MimS). The reduced modulus may have been related to interfacial hydrogen bonding and decreased cross-link density. Elongation at the breaking point consistently increased with MimS loading. Simultaneously, the tensile strength of the ultra deformation also increased substantially. There are two possible explanations for the altered mechanical performance. First, filler dispersion was largely improved by hydrogen bonding between the silica surface and the ion units in poly(MimS) and poly(SBR-g-MimS). Second, the interfacial bonding between silica and rubber was partially caused by hydrogen bonding, which may facilitate molecular mobility in the interfacial area. The facilitated chain mobility enables a higher degree of chain orientation, which is essential for the reinforcement of rubber.

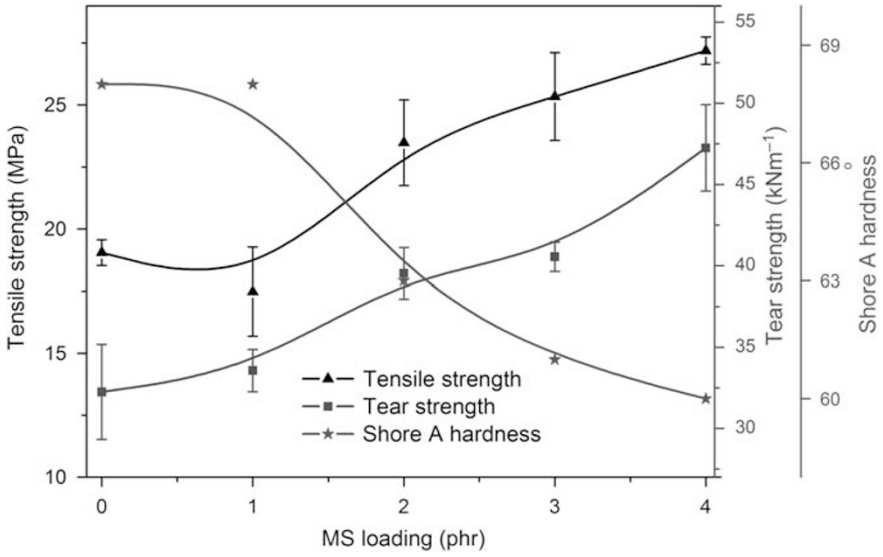

Figure 9 Mechanical comparisons of the SBR/silica vulcanizates. A full color version of this figure is available at *Polymer Journal* online.

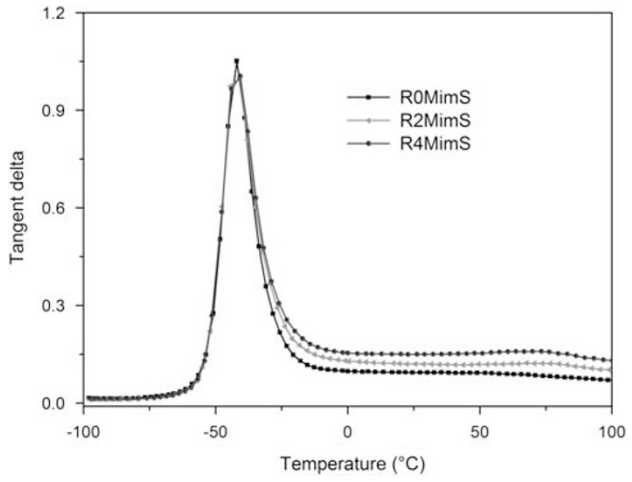

Figure 10 Dynamic mechanical comparisons of the SBR/silica vulcanizates. A full color version of this figure is available at *Polymer Journal* online.

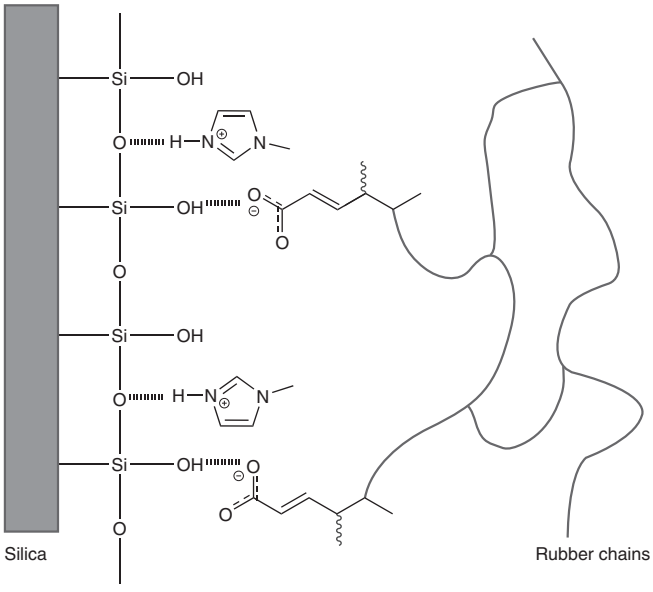

Figure 11 Schematic interfacial structure between silica and SBR chains. A full color version of this figure is available at *Polymer Journal* online.

Dynamic mechanical performance was also evaluated and is shown in Figure 10. The glass transition temperature (Tg) of the vulcanizates was practically unchanged. The compounds with MimS possessed a higher mechanical loss above Tg as compared with the unmodified sample. Interfacial interactions via non-covalent bonding such as the ionic bond or the hydrogen bond may lead to higher hysteresis. When the elastic sample ($T > Tg$) is loaded with dynamic strain, the rubber chains in the interfacial region may readily be deformed due to a weakened filler network and altered interfacial structures.[27,54] Aggravated interfacial chain motion then leads to higher loss at temperatures above the glass transition.

Suggested interfacial structure in SBR/silica/MimS composites

Owing to the described interaction between MimS and silica and MimS's reactivity to SBR chains, the MimS-modified SBR/silica interfacial structure may differ somewhat between uncured rubber compounds and the corresponding vulcanizates. The role of MimS in the vulcanizate is illustrated schematically in Figure 11. For interactions between MimS and silica (as revealed by gel formation, FTIR spectroscopy and the X-ray photon spectroscopy spectra), it is proposed that in uncured rubber compounds, MimS is strongly adsorbed onto the silica surface by hydrogen bonding between MimS and silica. Hydrogen bonding could restrain the filler network and facilitate filler dispersion due to weakened interactions among silica particles. After vulcanization, MimS molecules, which may have limited interactions with SBR chains because of their high polarity, can be chemically bonded to SBR chains via the graft product poly(SBR-g-MimS). Owing to this modified interface structure and improved filler dispersion, the greatly improved mechanical performance of SBR/silica composites was successfully achieved.

CONCLUSIONS

A novel functional IL, MimS, was successfully synthesized, characterized and explored as a modifier in an SBR/silica composite. MimS was found to be polymerized and/or grafted onto SBR molecules during vulcanization. The interactions between silica and the ionic units were substantiated to be hydrogen bonding. Both the cation and the anion

in the ionic unit could have been interacting with the silica surface via hydrogen bonding. The silica network in the rubber matrix was effectively restrained. Silica dispersion and the mechanical performance of the vulcanizates were effectively improved. The altered performance of the rubber compounds was related to altered filler dispersion and interfacial bonding, which originated from the reactivity of MimS with rubber chains and the hydrogen bonding between silica and the ionic unit induced by MimS.

ACKNOWLEDGEMENTS

We thank the National Natural Science Foundation of China (50873035, 50933005), Guangdong Natural Science Foundation (151008901000137) and Fundamental Research for the Central Universities (200922007) for their financial support.

1 Zhuravlev, L. T. The surface chemistry of amorphous silica. Zhuravlev Model. *Colloids Surf. A* **173,** 1–38 (2000).
2 Wolf, S. & Wang, M. J. Filler-elastomer interactions. Part IV. The effect of the surface energies of fillers on elasmomer reinforcement. *Rubber Chem. Technol.* **65,** 329–342 (1992).
3 Wang, M. J., Morris, M. D. & Kutsovsky, Y. Effect of fumed silica surface area on silicone rubber reinforcement. *Kautsch. Gummi Kunstst.* **61,** 107–117 (2008).
4 Wang, M. J. & Wolf, S. Filler-elastomer interactions. Part V. Investigation of the surface energies of silane-modified silicas. *Rubber Chem. Technol.* **65,** 715–735 (1992).
5 Jesionowski, T. & Krysztafkiewicz, A. Influence of silane coupling agents on surface properties of precipitated silicas. *Appl. Surf. Sci.* **172,** 18–32 (2001).
6 Wang, M. J. Effect of polymer-filler and filler-filler interactions on dynamic properties of filled vulcanizates. *Rubber Chem. Technol.* **71,** 519–589 (1997).
7 Liu, Y. H., Lin, H. P. & Mou, C. Y. Direct method for surface silyl functionalization of mesoporous silica. *Langmuir* **20,** 3231–3239 (2004).
8 Rao, A. V., Kulkarni, M. M., Amalnerkar, D. P. & Seth, T. Surface chemical modification of silica aerogels using various alkyl-alkoxy/chloro silanes. *Appl. Surf. Sci.* **206,** 262–270 (2003).
9 Earle, M. J., McCormac, P. B. & Seddon, K. R. Diels-Alder reactions in ionic liquids: a safe recyclable alternative to lithium perchlorate-diethyl ether mixtures. *Green Chem.* **1,** 23–25 (1999).
10 Huddleston, J. G., Visser, A. E., Reichert, W. M., Willauer, H. D., Broker, G. A. & Rogers, R. D. Characterization and comparison of hydrophilic and hydrophobic room temperature ionic liquids incorporating the imidazolium cation. *Green Chem.* **3,** 156–164 (2001).
11 Fuller, J., Carlin, R. T. & Osteryoung, R. A. The room temperature ionic liquid 1-ethyl-3-methylimidazolium tetrafluoroborate: electrochemical couples and physical properties. *J. Electrochem. Soc.* **144,** 3881–3886 (1997).
12 Fukushima, T., Kosaka, A., Ishimura, Y., Yamamoto, T., Takigawa, T., Ishii, N. & Aida, T. Molecular ordering of organic molten salts triggered by single-walled carbon nanotubes. *Science* **300,** 2072–2074 (2003).
13 Wu, B. H., Hu, D., Kuang, Y. J., Liu, B., Zhang, X. H. & Chen, J. H. Functionalization of carbon nanotubes by an ionic-liquid polymer: dispersion of Pt and PtRu nanoparticles on carbon nanotubes and their electrocatalytic oxidation of methanol. *Angew. andte Chem. Int. Ed.* **48,** 4751–4754 (2009).
14 Scheeren, C. W., Machado, G., Dupont, J., Fichtner, P. F. & Texeira, S. R. Nanoscale Pt(0) particles prepared in imidazolium room temperature ionic liquids: synthesis from an organometallic precursor, characterization, and catalytic properties in hydrogenation reactions. *Inorg. Chem.* **42,** 4738–4742 (2003).
15 Nakashima, T. & Kimizuka, N. Interfacial synthesis of hollow TiO2 micropheres in ionic liquids. *J. Am. Chem. Soc.* **125,** 6386–6387 (2003).
16 Li, Z. H., Liu, Z. M., Zhang, J. L., Han, B. X., Du, J. M., Gao, Y. N. & Jiang, T. Synthesis of single-crystal gold nanosheets of large size in ionic liquids. *J. Phys. Chem. B* **109,** 14445–14448 (2005).
17 Zhou, Y. & Antonietti, M. A series of highly ordered, super-microporous, lamellar silicas prepared by nanocasting with ionic liquids. *Chem. Mater.* **16,** 544–550 (2004).
18 Trewyn, B. G., Whitman, C. M. & Lin, V. S. Morphological control of room-temperature ionic liquid templated mesoporous silica nanoparticles for controlled release of antibacterial agents. *Nano lett.* **4,** 2139–2143 (2004).
19 Zhang, J., Ma, Y. B., Shi, F., Liu, L. Q. & Deng, Y. Q Room temperature ionic liquids as templates in the synthesis of mesoporous silica via a sol-gel method. *Microporous Mesoporous Mater.* **119,** 97–103 (2009).
20 Zhou, Y., Schattka, J. H. & Antonietti, M. Room-temperature ionic liquids as template to monolithic mesoporous silica with wormlike pores via a sol–gel nanocasting technique. *Nano Lett.* **4,** 477–481 (2004).
21 Guo, B. C., Liu, X. L., Lei, Y. D. & Jia, D. M. Adsorption of ionic liquid onto halloysite nanotubes: mechanism and reinforcement of the modified clay to rubber. *J. Macromol. Sci., Phys.* (accepted).
22 Dupont, J. & Suarezb, P. A. Physico-chemical processes in imidazolium ionic liquids. *Phys. Chem. Chem. Phys.* **8,** 2441–2452 (2006).
23 Winterton, N. Solubilization of polymers by ionic liquids. *J. Mater. Chem.* **16,** 4281–4293 (2006).
24 Marwanta, E., Mizumo, T., Nakamura, N. & Ohno, H. Improved ionic conductivity of nitrile rubber/ionic liquid composites. *Polymer* **46,** 3795–3800 (2005).
25 Guo, B. C., Chen, F., Lei, Y. D., Liu, X. L., Wan, J. J. & Jia, D. M. Styrene-butadiene rubber/halloysite nanotubes nanocomposites modified by sorbic acid. *Appl. Surf. Sci.* **255,** 7329–7336 (2009).
26 Guo, B. C., Chen, F., Lei, Y. D. & Jia, D. M. Tubular clay composites with high strength and transparency. *J. Macromol. Sci., Part B: Phys.* **49,** 111–121 (2010).
27 Guo, B. C., Chen, F., Lei, Y. D. & Chen, W. W. Significantly improved performance of rubber/silica composites by addition of sorbic acid. *Polym. J.* **42,** 319–326 (2010).
28 Belieres, J. P. & Angell, C. A. Protic ionic liquids: Preparation, characterization, and proton free energy level representation. *J. Phys. Chem. B* **111,** 4926–4937 (2007).
29 Nakamoto, H. & Watanabe, M. Bronsted acid-base ionic liquids for fuel cell electrolytes. *Chem. Commun.* **24,** 2539–2541 (2007).
30 Johansson, K. M., Izgorodina, E. I., Forsyth, M., MacFarlane, D. R. & Seddon, K. R. Protic ionic liquids based on the dimeric and oligomeric anions: (AcO)(x)Hx-1(−). *Phys. Chem. Chem. Phys.* **10,** 2972–2978 (2008).
31 Fernicola, A., Panero, S. & Scrosati, B. Proton-conducting membranes based on protic ionic lquids. *J. Power Sources* **178,** 591–595 (2008).
32 Pernak, J., Goc, I. & Mirska, I. Antimicrobial activities of protic ionic liquids with lactate anion. *Green Chem.* **6,** 323–329 (2004).
33 Baca, S. G., Filippova, I. G., Gherco, O. A., Gdaniec, M., Simonov, Y. A., Gerbeleu, N. V., Franz, P., Basler, R. & Decurtins, S. Nickel(II), Cobalt(II), Copper(II), and Zinc(II)-phthalate and 1-methylimidazole coordination compounds: synthesis, crystal structures and magnetic properties. *Inorg. Chim. Acta* **357,** 3419–3429 (2004).
34 Chu, S. D., Hawes, J. W. & Lorigan, G. A. Solid-state NMR spectroscopic studies on the interaction of sorbic acid with phospholipid membranes at different pH levels. *Magn. Reson. Chem.* **47,** 651–657 (2009).
35 Nakamoto, H., Noda, A., Hayamizu, K., Hayashi, S., Hamaguchi, H. & Watanabe, M. Proton-conducting properties of a bronsted acid-base ionic liquid and ionic melts consisting of bis(trifluoromethanesulfonyl)imide and benzimidazole for fuel cell electrolytes. *J. Phys. Chem. C* **111,** 1541–1548 (2007).
36 Rajkumar, T. & Rao, G. R. Synthesis and characterization of hybrid molecular material prepared by ionic liquid and silicotungstic acid. *Mater. Chem. Phys.* **112,** 853–857 (2008).
37 Jerman, I., Jovanovski, V., Šurca Vuk, A., Hoèevar, S. B., Gaberšèek, M., Jesih, A. & Orel, B. Ionic conductivity, infrared and raman spectroscopic studies of 1-methyl-3-propylimidazolium iodide ionic liquid with added iodine. *Electrochim. Acta* **53,** 2281–2288 (2008).
38 Šurca Vuka, A., Jovanovskia, V., Pollet-Villardb, A., Jermana, I. & Orela, B. Imidazolium-based ionic liquid derivatives for application in electrochromic devices. *Sol. Energy Mater. Sol. Cells* **92,** 126–135 (2008).
39 Doiuchi, T., Dodoh, T. & Yamaguchi, H. Asymmetric radical polymerization of (-)-3-p-menthyl sorbate. *Makromol. Chem.* **191,** 1253–1260 (1990).
40 Weng, Y. M., Chen, M. J. & Chen, W. Antimicrobial food packaging materials from poly(ethylene-co-methacrylic acid). *Food Sci. Technol.* **32,** 191–195 (1999).
41 Watts, J. F. & Wolstenholme, J. An introduction to surface analysis by XPS and AES. *Chapter* **5,** 149–156 (2003).
42 Guo, B. C., Lei, Y. D., Chen, F., Liu, X. L., Du, M. L. & Jia, D. M. Styrene–butadiene rubber/halloysite nanotubes nanocomposites modified by methacrylic acid. *Appl. Surf. Sci.* **255,** 2715–2722 (2008).
43 Paparazzo, E. On the XPS analysis of Si-OH groups at the surface of silica. *Surf. Interface Anal.* **24,** 729–730 (1996).
44 Payne, A. R. The dynamic properties of carbon black-loaded natural rubber vulcanizates. II. *J. Appl. Polym. Sci.* **6,** 368–372 (1962).
45 Null, V. Safe process oils for tires with low environmental impact. *Kautsch. Gummi Kunstst.* **52,** 799–805 (1999).
46 Ishizaki, M. & Matsutani, Y. High damping rubber composition for damping component, is formed by mixing softener chosen from liquid rubber, paraffin and naphthene oil, rubber base, silane compound, carbon black and silica, each having content of preset range. JP2009030016-A (2009).
47 Lin, Y. C., Lee, W. J., Chen, S. J., Chang-Chien, G. P. & Tsai, P. J. Characterization of PAHs exposure in workplace atmospheres of a sinter plant and health-risk assessment for sintering workers. *J. Hazard. Mater.* **158,** 636–643 (2008).
48 Matsumoto, A., Nagahama, S. & Odani, T. Design and polymer structure control based on polymer crystal engineering. topochemical polymerization of 1,3-diene mono- and dicarboxylic acid derivatives bearing a naphthylmethylammonium group as the countercation. *J. Am. Chem. Soc.* **122,** 9109–9119 (2000).
49 Taketani, S. & Matsumoto, A. Facile synthesis of a degradable gel by radical copolymerization of vinyl sorbate and molecular oxygen. *Macromol. Chem. Phys.* **205,** 2451–2456 (2004).
50 Yamaguchi, H., Tetsuroh, I., Toshio, H. & Doiuchi, T. Asymmetric induction polymerization of monomer salts prepared from 1,3-butadiene-l-carboxylic acid and optically active amines. *Makromol. Chem.* **191,** 1243–1251 (1990).
51 Yu, J. J. & Ryu, S. H. Ultraviolet-initiated photografting of glycidyl methacrylate onto styrene–butadiene rubber. *J. Appl. Polym. Sci.* **73,** 1733–1739 (1999).
52 Romero-Sanchez, M. D., Pastor-Blas, M. M. & Martin-Martinez, J. M. Adhesion improvement of SBR rubber by treatment with trichloroisocyanuric acid solutions in different esters. *Int. J. Adhes. Adhes.* **21,** 325–337 (2001).
53 Innocenzi, P. Infrared spectroscopy of sol-gel derived silica-based films: a spectra-microstructure overview. *J. Non-Cryst. Solids* **316,** 309–319 (2003).
54 Sato, K. Ionic crosslinking of carboxylated SBR. *Rubber Chem. Technol.* **56,** 942–958 (1983).